ARTICLE

Internal Conversion Process of Chlorophyll a in Solvents in Femtosecond Pump-Probe Laser Fields

Kai Niu, Li-qing Dong, Shu-lin Cong*

Department of Physics, Dalian University of Technology, Dalian 116024, China

(Dated: Received on October 10, 2007; Accepted on December 22, 2007)

The internal conversion (IC) processes of chlorophyll a (chl-a) in solvents are studied based on the reduced density matrix theory. The IC times can be obtained by simulating the experimental fluorescence depletion spectra (FDS). The calculated IC times of chl-a in ethyl acetate, tetrahydrofuran and dimethyl formamide are 141, 147, and 241 fs, respectively. The oscillation feature of the FDS results from the forward and backward transfer of the population between coupled electronic states. The effects of diabatic coupling between two electronic states on the IC time and the FDS are described. The influence of molecule-reservoir coupling on the IC time is also investigated.

Key words: Fluorescence depletion spectrum, Internal conversion, Reduced density matrix

I. INTRODUCTION

The internal conversion (IC) dynamics of molecules in solutions has attracted great interest among researchers recently. Various techniques have been developed to determine molecular IC rates and pathways, such as femtosecond time-resolved photoelectron spectroscopy [1,2], femtosecond transient absorption [3], fluorescence up-conversion technique [4], and femtosecond time-resolved stimulated emission pumping fluorescence depletion spectrum (FDS) [5-11]. Seideman *et al.* studied theoretically the dynamics of a radiationless transition of pyrazine molecule based on a nonperturbative quantum mechanical theory [12]. May *et al.* studied the transient absorption of the LH2 antenna system and incorporated exciton-exciton annihilation processes using the multiexciton density matrix theory [13,14]. Based on the Redfield theory of relaxation, Jean *et al.* developed a quantum theoretical model used for describing the photoinduced electron transfer and the molecular IC process [15]. Domcke *et al.* [16] and Mukamel *et al.* [17] used the so-called nonlinear susceptibility approach, and Lin *et al.* used the non-equilibrium linear susceptibility approach to analyse the femtosecond pump-probe experiments [18,19]. He *et al.* described theoretically the fluorescence depletion spectrum of dye molecules [20]. In previous work, we calculated the femtosecond FDSs of dye oxazine 750 and rhodamine 700 molecules in acetone and discussed the IC dynamics of chlorophyll a (chl-a) in aprotic solvents using a simplified theoretical model based on the perturbative density operator method and the transient linear susceptibility theory [21-24].

In the present work, we describe more precisely the femtosecond time-resolved FDS involving IC process. As illustrative examples, the FDSs and IC times of chl-a in ethyl acetate (EA), tetrahydrofuran (THF) and dimethyl formamide (DMF) are calculated. By fitting our model to the experimental FDSs measured by Shi *et al.* [8], we obtain the IC times of chl-a in the three solutions and interpret the oscillation features of the FDSs. The effects of the diabatic coupling between two electronic states on the FDS and the IC time are described. The influence of molecule-reservoir coupling on the IC time is also discussed.

II. THEORETICAL METHOD

The FDS developed by Kong *et al.* has been described in many works [6,7,10,20]. Only an outline is given here. Figure 1 illustrates the schematic diagram of the fluorescence depletion experiment involving the IC process [8]. The molecule is firstly excited from S_0

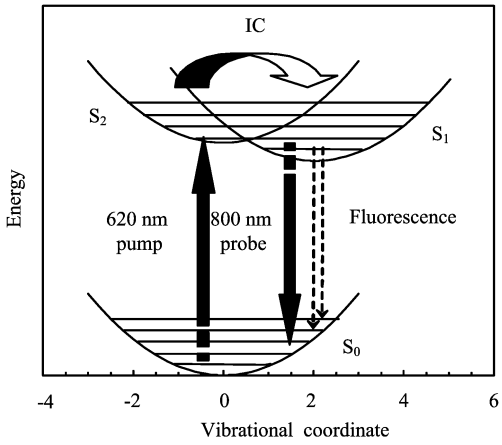

FIG. 1 Schematic diagram of the fluorescence depletion involving the IC process.

*Author to whom correspondence should be addressed. E-mail: shlcong@dlut.edu.cn

to S_2 states by a pump laser. The population of the S_2 state is transferred to the higher vibrational level of the S_1 state through an IC process. Then a vibrational relaxation process occurs in the S_1 state. After a delay time, a probe pulse induces a stimulated emission from the S_1 state to the S_0 state, which weakens the fluorescence intensity from the S_1 state. The FDS reflects the IC and the vibrational relaxation dynamic processes occurring in the excited states. We can abstract the useful information about the IC process from the calculated FDSs.

The FDS intensity $I_{\rm FDS}$ can be expressed as [20,25,26]

$$I_{\rm FDS} = -2\omega_{\rm pr}\int_{-\infty}^{\infty} {\rm d}t {\rm Im}[E^*_{\rm pr}(t)P_{\rm pr}(t)]\cdot \{1+C_1[1-\exp(-kt)]\} \quad (1)$$

The expression in the curly brace is related to the excited solvation [20], where C_1 reflects the relative contribution of the solvation effect and k denotes the slower decay rate constant caused by the solvation effect. $E_{\rm pr}(t)$ and $\omega_{\rm pr}$ are the envelope and the carrier frequency of the probe pulse, respectively. The polarization $P(t)$ induced by the probe pulse is calculated by [27]

$$P(t) = {\rm Tr_s}\{\Omega[\sigma^{\rm pu+pr}(t)-\sigma^{\rm pu}(t)]\} \quad (2)$$

where $\rm Tr_s$ denotes the trace with respect to the molecular degrees of freedom. Ω is the molecular transition dipole moment and is defined by Eq.(11). $\sigma^{\rm pu+pr}(t)$ and $\sigma^{\rm pu}(t)$, whose expressions are calculated by Eq.(15), represent the reduced density matrices with and without the probe pulse, respectively. The polarization envelope of the probe pulse $P_{\rm pr}(t)$ can be expressed in a single Fourier component as [26]

$$P_{\rm pr}(t)\exp(-i\omega_{\rm pr}t)=n_d\sum_{\kappa\lambda}[\sigma^{\rm pu+pr}_{\kappa\lambda}(t)-\sigma^{\rm pu}_{\kappa\lambda}(t)]\Omega_{\lambda\kappa} \quad (3)$$

where $\Omega_{\lambda\kappa}$ is the transition dipole moment between the electronic states $|\lambda\rangle$ and $|\kappa\rangle$, and $n_{\rm d}$ is the number-density of the solute molecules.

The total Hamiltonian of a system which is composed of molecules and a reservoir is written as

$$\begin{aligned} H_{\rm T} &= H_{\rm S}+H_{\rm S-E}+H_{\rm R}+H_{\rm S-R} \\ H_{\rm S} &= \sum_{a,b}(\delta_{ab}H_{ab}+V_{ab})|a\rangle\langle b| \\ H_{aa} &= T_{\rm vib}+U_a(Q) \end{aligned} \quad (4)$$

where $H_{\rm S}$ is the active molecular Hamiltonian, H_{aa} is the diagonal part of $H_{\rm S}$, $T_{\rm vib}$ and $U_a(Q)$ are the molecular kinetic and potential energy operators, respectively. Here, a minimal model containing a single harmonic coordinate is used. As May *et al.* did [28-30], the potential energy operator is written as

$$U_a(Q) = U_a^{(0)}+\frac{\hbar\omega_{\rm vib}}{2}(Q-Q_a^{(0)})^2 \quad (5)$$

where $U_a^{(0)}$ denotes the reference energy of electronic state $|a\rangle$. $\omega_{\rm vib}$ is molecular vibrational frequency, and $Q_a^{(0)}$ is the shift of the potential energy surface (PES) along the dimensionless position coordinate Q. In a more accurate treatment, multiple vibrational modes as well as damping of the vibrational motion caused by molecule-environment interaction should be taken into account [31-33]. Here, for simplicity, a single averaged vibrational coordinate is used in the calculation.

The off-diagonal part $V_{ab}=\langle a|V(Q)|b\rangle$ of $H_{\rm S}$ represents the coupling between the diabatic states $|a\rangle$ and $|b\rangle$, where $V(Q)$ is given by [34-36]

$$V(Q) = A\exp[-B(Q-Q_0)^2] \quad (6)$$

where A is the reference value of the inter-site coupling and B serves the characteristic inverse length determined by the wave function overlapping. Q_0 denotes the crossing point of the two diabatic states. According to Eq.(5), Q_0 can be obtained by solving

$$U_1(Q_0) = U_2(Q_0) \quad (7)$$

$$U_1^{(0)}+\frac{\hbar\omega_{\rm vib}}{2}(Q_0-Q_1^{(0)})^2 = U_2^{(0)}+\frac{\hbar\omega_{\rm vib}}{2}(Q_0-Q_2^{(0)})^2 \quad (8)$$

$$Q_0 = \frac{Q_1^{(0)}+Q_2^{(0)}}{2}+\frac{U_1^{(0)}-U_2^{(0)}}{\hbar\omega_{\rm vib}(Q_1^{(0)}-Q_2^{(0)})} \quad (9)$$

For the present PES model, no vibrational level of the S_2 state is below the crossing point of S_1 and S_2. This guarantees an accurate temporal evolution of the population in the diabatic representation [37].

$H_{\rm R}$ in Eq.(4) denotes the Hamiltonian of reservoir consisting of an ensemble of harmonic oscillators in thermal equilibrium. Its expression can be found in Refs.[28,38-41]. The molecule-reservoir interaction $H_{\rm S\text{-}R}$ can be factorized into $H_{\rm S\text{-}R}$=$K(Q)\phi(Z)$, where $K(Q)$ and $\phi(Z)$ are the molecular part and the reservoir part, respectively, and Z=$\{Z_\xi\}$ denotes a set of reservoir degrees of freedom.

The interaction $H_{\rm S\text{-}E}$ of the molecule with the laser field is written as

$$H_{\rm S-E}(t) = -\Omega E(t) \quad (10)$$

$$\Omega = \sum_{a\neq b} d_{ab}|a\rangle\langle b| \quad (11)$$

where d_{ab} is the transition dipole moment between $|a\rangle$ and $|b\rangle$ [28].

The laser field $E(t)$ can be written as

$$E(t) = \sum_{\rm s=pu,pr} E_{\rm s}(t)\exp(-i\omega_{\rm s}t)+c.c. \quad (12)$$

where $\omega_{\rm s}$ is the pump (or probe) laser carrier frequency. $E_{\rm s}(t)$, the envelope of the pump (or probe) pulse with a Gaussian shape, is given by

$$E_{\rm s}(t) = F_{\rm s}\exp\left[-4\ln 2\left(\frac{t-t_{\rm s}}{T_{\rm s}}\right)^2\right] \quad (13)$$

DOI:10.1088/1674-0068/21/03/211-216

where F_s is the electric field amplitude of the pump (or probe) laser pulse. t_s is the central time and T_s denotes a full-width at half maximum (FWHM) of the pump (or probe) pulse. The delay time between the pump and the probe pulses is t_{pu}-t_{pr}.

The population evolution of molecule in liquids is calculated by using the well-known Liouville-von-Neumann equation

$$\frac{\partial}{\partial t}\rho(t) = -\frac{i}{\hbar}[H_T, \rho(t)] \tag{14}$$

where $\rho(t)$ denotes the density matrix of the system. The reduced density matrix is defined as $\sigma(t)$=$\mathrm{Tr_R}\{\rho(t)\}$, where the trace is performed over reservoir degrees of freedom. In the Markovian approximation, the time evolution of reduced density matrix is determined by [35,38,42-44].

$$\begin{aligned}\frac{\partial}{\partial t}\sigma_{\mu\nu}(t) &= -i\omega_{\mu\nu}\sigma_{\mu\nu}(t) - \frac{i}{\hbar}[V, \sigma(t)]_{\mu\nu} - \\ &\quad \frac{i}{\hbar}E(t)[\Omega, \sigma(t)]_{\mu\nu} + \left[\frac{\partial}{\partial t}\sigma_{\mu\nu}(t)\right]_{\mathrm{diss}}\end{aligned} \tag{15}$$

where the Greek letters $|\mu\rangle$= $|a, M\rangle$ represent the eigenstates of H_S, and M is the vibrational quantum number. $\sigma_{\mu\nu}(t)$=$\langle\mu|\sigma(t)|\nu\rangle$ are the matrix elements of the reduced density matrix in the eigenstate representation. The transition frequencies $\omega_{\mu\upsilon}$ satisfy the relations $\omega_{\mu\nu}$=$(E_\mu - E_\nu)/\hbar$, with E_μ and E_ν being the eigenvalues of H_S. The total population on the ath PES, $P_a(t)$, is given by

$$P_a(t) = \sum_M \sigma_{aM,aM}(t) \tag{16}$$

In Eq.(15), the dissipative part $\left[\frac{\partial}{\partial t}\sigma_{\mu\nu}(t)\right]_{\mathrm{diss}}$ is related to the molecule-reservoir interaction. It can be expressed as [28,35]

$$\left[\frac{\partial}{\partial t}\sigma_{\mu\nu}(t)\right]_{\mathrm{diss}} = -\sum_{\kappa,\lambda} R_{\mu\nu\kappa\lambda}\sigma_{\kappa\lambda}(t) \tag{17}$$

where R is the Redfield tensor [35,45] and reads

$$\begin{aligned}R_{\mu\nu\kappa\lambda} &= -\Gamma_{\lambda\nu\mu\kappa}(\omega_{\kappa\mu}) - \Gamma_{\kappa\mu\nu\lambda}(\omega_{\lambda\nu}) + \\ &\quad \delta_{\lambda\nu}\sum_{\lambda'}\Gamma_{\mu\lambda'\lambda'\kappa}(\omega_{\kappa\lambda'}) + \\ &\quad \delta_{\kappa\mu}\sum_{\lambda'}\Gamma_{\nu\lambda'\lambda'\lambda}(\omega_{\lambda\lambda'})\end{aligned} \tag{18}$$

$$\begin{aligned}\Gamma_{\kappa\lambda\mu\nu}(\omega) &= \delta_{ab}\delta_{cd}\pi[1+n(\omega)]J(\omega)\cdot \\ &\quad \langle\kappa|Q - Q_a^{(0)}|\lambda\rangle\langle\mu|Q - Q_c^{(0)}|\nu\rangle\end{aligned} \tag{19}$$

here, we assume a molecule-reservoir coupling is bilinear in the coordinates [28,35,41], i.e.,

$$\begin{aligned}K(Q) &= \sum_a (Q - Q_a^{(0)})|a\rangle\langle a| \\ &= \sum_a \Delta Q_a|a\rangle\langle a|\end{aligned} \tag{20}$$

$$\phi(Z) = \sum_\xi \hbar k_\xi Z_\xi \tag{21}$$

$n(\omega)$ presents the Bose-Einstein distribution. $J(\omega)$ is the spectral density of the reservoir oscillators, which can be written as

$$J(\omega) = \sum_\xi k_\xi^2[\delta(\omega - \omega_\xi) - \delta(\omega + \omega_\xi)] \tag{22}$$

k_ξ is a coupling constant between the harmonic oscillator and the ξth degree of freedom of the reservoir. In the calculation, we take G=$2\pi J(\omega)$ as an adjustable parameter to describe the molecule-reservoir interaction. The vibrational life-time τ_μ of level μ is given by

$$\frac{1}{\tau_\mu} = 2\sum_\nu \Gamma_{\mu\nu\nu\mu}(\omega_{\mu\nu}) \tag{23}$$

In the present model, it reads [28]

$$\frac{1}{\tau_\mu} = [(1+2M)n(\omega) + M]G \tag{24}$$

The IC rate can be expressed as [15]

$$k_{\mathrm{IC}} = \frac{1}{\tau_{\mathrm{IC}}} \tag{25}$$

where τ_{IC} is the IC time. It equals to the time that the population of S_2 state decays to $1/e$ of its peak value.

III. NUMERICAL CALCULATIONS AND DISCUSSION

In the following, we use the above theory to calculate the FDSs and the IC times of chl-a in EA, THF and DMF. The experimental FDSs were measured by Shi *et al.* [8].

Figure 2 shows the femtosecond time-resolved FDSs at room temperature. The interesting parameters are obtained by fitting our calculations to the FDSs. The calculated IC times are 141, 147, and 241 fs for chl-a in EA, THF, and DMF, respectively. Three processes are found from the time-resolved FDSs: (i) an IC process with a few hundreds of femtoseconds, (ii) a faster decay process with a few hundreds of femtoseconds, and (iii) a slower decay process with a picosecond time scale. The IC process arises from the coupling between vibrational states [46]. The faster decay process depends on the solute molecules and reflects the vibrational relaxation time in the S_1 state. The slower decay process depends on the solvent used, and reflects the excited solvation

DOI:10.1088/1674-0068/21/03/211-216

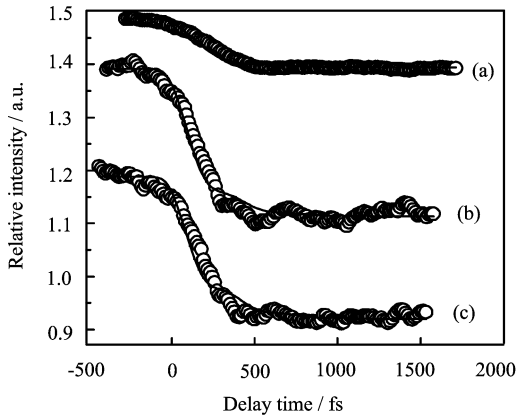

FIG. 2 Time-resolved fluorescence depletion spectra of chl-a in DMF (a), THF (b), and EA (c). Open circles show experimental data [8] and solid lines denote simulated results.

TABLE I The PES parameters of chl-a in different solvents, $U_a^{(0)}$ and $\omega_{\rm vib}$ are in $\rm cm^{-1}$

Solvent	PES	$Q_a^{(0)}$	$U_a^{(0)}$	$\omega_{\rm vib}$	$A(\hbar\omega_{\rm vib})$	B
EA	S_0	0	0	1250		
	S_1	2.2	14850	1250		
	S_2	0	16100	1250	0.31	15.1
THF	S_0	0	0	1250		
	S_1	2.2	14850	1250		
	S_2	0	16100	1250	0.31	15.8
DMF	S_0	0	0	1250		
	S_1	2.2	14850	1250		
	S_2	0	16100	1250	0.21	16.0

TABLE II The laser pulse parameters used in the calculations

Laser	$\omega_{\rm s}$/nm	FWHM/fs	Band width/nm
Pump pulse	620	100	10
Probe pulse	800	130	10

effect. From the experimental data of absorption and fluorescence spectra [47], we estimate the 0-0 transitions of $S_0 \rightarrow S_1$ and $S_0 \rightarrow S_2$ for chl-a to be at about 14850 and 16100 $\rm cm^{-1}$, respectively. In the calculations, the vibrational frequency is taken as 1250 $\rm cm^{-1}$ [22,48] and four vibrational levels are considered in each electronic state. The best fitted parameters for chl-a in the three solvents are collected in Table I. As the transition dipole moment between S_0 and S_1 (or S_0 and S_2) of chl-a is not exactly known, they are taken as 1 atomic unit, although their values are different. For simplicity, we neglect the laser-induced transition between S_1 and S_2 states. The laser pulse parameters listed in Table II are the same as those used in experiment [8]. The electric field amplitudes of the pump and probe pulses are 0.5×10^{-3} and 1.5×10^{-3} a.u., respectively.

It can be seen from Fig.2 that the oscillations appear in the calculated and experimental FDSs for chl-a in

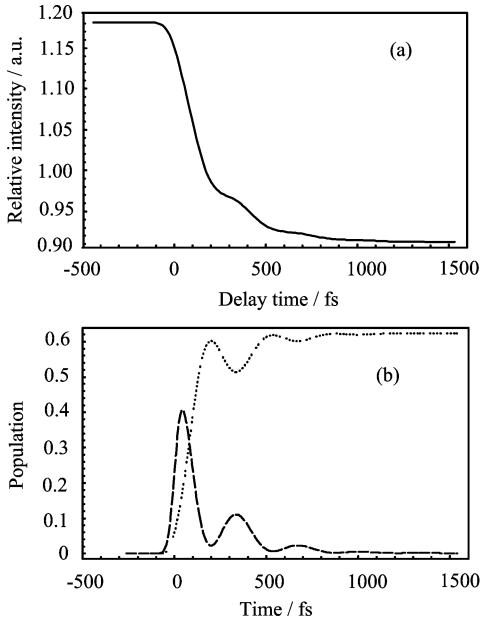

FIG. 3 (a) The calculated FDS for chl-a in EA and (b) the temporal population evolutions of the S_1 (dotted line) and S_2 (dashed line) states when the probe pulse is switched off.

EA and THF. In order to interpret this phenomenon, in Fig.3 we show the calculated FDS for chl-a in EA and the population evolutions of S_1 and S_2 states. The population of S_1 or S_2 state is calculated according to Eq.(16) under the condition in which the probe pulse is switched off. Since the FDS intensity is proportional to the population of S_1 state, the oscillations of the FDS result from the population oscillations between S_1 and S_2 states. We can estimate from Fig.3 that the oscillation period for chl-a in EA is about 250 fs. It is seen from Fig.2 that the oscillation period between S_1 and S_2 states for chl-a in THF is also about 250 fs.

The PESs of S_1 and S_2 states and the coupling between the two states for chl-a in EA are illustrated in Fig.4. The solid and dashed lines show the PESs in the adiabatic and diabatic representations, respectively, and the dotted line presents the diabatic coupling $V(Q)$ in Eq.(6) versus vibrational coordinate. The population of the S_2 state can be transferred to the S_1 state via the diabatic coupling.

We now discuss the effects of the parameters A and B on the IC time and the FDS intensity. The parameter A in Eq.(6) denotes the maximum value of the diabatic coupling between the S_1 and S_2 states. The IC time decreases with the increase of A. The parameter B reflects the width of distribution curve of the potential coupling $V(Q)$. When B increases, the effective coordinate range of $V(Q)$ decreases, and the IC time increases. Figure 5 shows the FDSs of chl-a in EA for different coupling parameters (A and B). The calculated IC times are 156, 141 and 132 fs for $A = 0.29$, 0.31 and 0.33 $\hbar\omega_{\rm vib}$ at $B =$ 15.1, respectively. The IC times are 139, 141, and 144 fs

DOI:10.1088/1674-0068/21/03/211-216

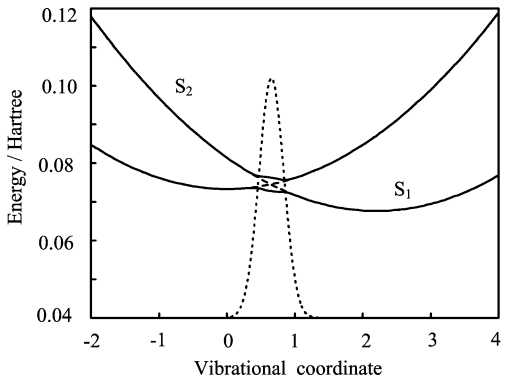

FIG. 4 The PESs of S_1 and S_2 states and their coupling intensity for chl-a in EA. The dashed lines show the PESs of the molecule in the diabatic representation. The solid lines show the PESs of the molecule in the adiabatic representation. The dotted line denotes the diabatic coupling $V(Q)$ in Eq.(6) versus vibrational coordinate.

for B=14.0, 15.1, and 16.0 at $A = 0.31\ \hbar\omega_{\rm vib}$, respectively. When A increases or B decreases, the IC time decreases, and the population transfer rate from the S_2 state to the S_1 state becomes faster. When the delay time is less than 150 fs, as shown in the insets of Fig.5, the FDS intensity increases slightly with the decrease of the IC time. However, when the delay time is larger than 150 fs, the FDS intensity decreases slightly with the decrease of the IC time. This can be interpreted as follows. The frequency of pump pulse is nearly resonant with the transition from $|2,0\rangle$ to $|0,0\rangle$. When A increases or B decreases, the ground vibrational level of the S_2 state has a larger shift, which reduces the population pumped to the S_2 state and therefore weakens the FDS intensity when the delay time is larger than 150 fs.

When the molecule-reservoir coupling parameter G increases, the vibrational relaxation rate of the S_2 state will increase, as shown in Eq.(24). The population taking part in the vibrational relaxation process will increase, and the population participating in the IC process will decrease. Thus, the IC time increases with the increase of G. The best fitted values of G are 0.041, 0.046, and 0.045 $\hbar\omega_{\rm vib}$ for chl-a in EA, THF, and DMF, respectively. The vibrational relaxation rates can be calculated using Eq.(24) and are proportional to G. The parameter C_1 in Eq.(1) reflecting the relative contribution of the solvation effect is taken as 0.06 for chl-a in the three solvents. The slower decay rate constant k depends on the viscosity of the solvent [20]. The k value decreases with the increase of the solvent viscosity. The best fitted values are 0.07, 0.06, and 0.04 $\rm ps^{-1}$ for chl-a in EA, THF, and DMF, respectively.

Compared with what was in our previous work [22], the present model has the following advantages. (i) The oscillation features of the FDS can be simulated. (ii) The relaxation between vibrational levels is treated using a bilinear way, while Ref.[22] used a step relaxation model. (iii) The shapes of the laser pulses can be taken into account in the model calculation.

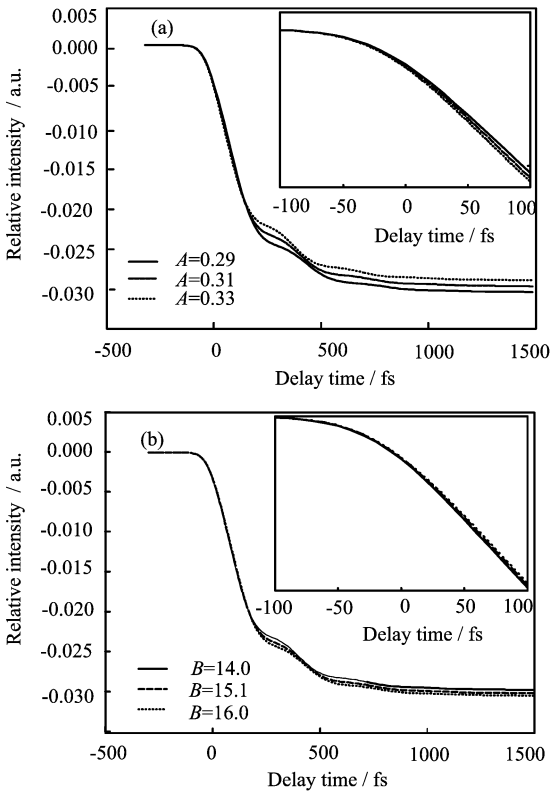

FIG. 5 Time-resolved fluorescence depletion spectra of chl-a in EA for different A and B. (a) A=0.29 $\hbar\omega_{\rm vib}$ (solid line), 0.31 $\hbar\omega_{\rm vib}$ (dashed line), and 0.33 (dotted line) $\hbar\omega_{\rm vib}$ at B=15.1. (b) B=14.0 (solid line), 15.1 (dashed line), and 16.0 (dotted line) at $A = 0.31\ \hbar\omega_{\rm vib}$. The other parameters are the same as those in Fig.2.

IV. CONCLUSION

In this work, we studied the internal conversion processes of chlorophyll a in solvents based on the reduced density matrix theory. From the theoretical simulations of the fluorescence depletion spectra, we determine the internal conversion times of chlorophyll a in ethyl acetate, tetrahydrofuran and dimethyl formamide to be 141, 147, and 241 fs, respectively. The oscillations appearing in the fluorescence depletion spectra for chl-a in EA and THF result from the forward and backward transfer of the population between S_1 and S_2 states, and the oscillation periods are about 250 fs. The effects of the diabatic coupling between two electronic states on the internal conversion time and fluorescence depletion spectrum are discussed. With the increase of the intersite coupling parameter A, the internal conversion time decreases and the fluorescence depletion intensity in a large delay time region decreases. When the character-

DOI:10.1088/1674-0068/21/03/211-216

istic inverse length B increases, the internal conversion time increases and the fluorescence depletion intensity in a large delay time region increases. With the increase of the molecule-reservoir coupling, the internal conversion time will increase.

V. ACKNOWLEDGMENTS

We would like to thank Dr. Y. Shi and Professor K. L. Han for providing the FDS data and useful discussions. K. Niu is grateful to Professor V. May for enlightening suggestions. This work was supported by the National Natural Science Foundation of China (No.10674022 and No.20633070).

[1] V. Blanchet, M. Z. Zgierski, T. Seideman, and A. Stolow, Nature **401**, 52 (1999).
[2] A. Stolow, Ann. Rev. Phys. Chem. **54**, 89 (2003).
[3] P. M. Hare, C. E. Crespo-Hernández, and B. Kohler, Proc. Natl. Acad. Sci. USA **104**, 435 (2007).
[4] N. Mataga, Y. Shibata, H. Chosrowjan, N. Yoshida, and A. Osuka, J. Phys. Chem. B **104**, 4001 (2000).
[5] J. Y. Liu, W. H. Fan, K. L. Han, W. Q. Deng, D. L. Xu, and N. Q. Lou, J. Phys. Chem. A **107**, 10857 (2003).
[6] J. Y. Liu, W. H. Fan, K. L. Han, D. L. Xu, and N. Q. Lou, J. Phys. Chem. A **107**, 1914 (2003).
[7] G. J. Zhao, J. Y. Liu, L. C. Zhou, and K. L. Han, J. Phys. Chem. B **111**, 8940 (2007).
[8] Y. Shi, J. Y. Liu, and K. L. Han, Chem. Phys. Lett. **410**, 260 (2005).
[9] Y. Shi, J. Y. Liu, K. L. Han, and N. Q. Lou, Chin. J. Chem. Phys. **17**, 1 (2004).
[10] Q. Zhong, Z. Wang, Y. Liu, Q. Zhu, and F. Kong, J. Chem. Phys. **105**, 5377 (1996).
[11] Q. Zhong, Z. Wang, Y. Sun, Q. Zhu, and F. Kong, Chem. Phys. Lett. **248**, 277 (1996).
[12] Y. Suzuki, M. Stener, and T. Seideman, J. Chem. Phys. **118**, 4432 (2003).
[13] B. Brüggemann and V. May, J. Chem. Phys. **120**, 2325 (2004).
[14] T. Renger, V. May, and O. Kühn, Phys. Rep. **343**, 137 (2001).
[15] J. M. Jean, R. A. Friesner, and G. R. Fleming, J. Chem. Phys. **96**, 5827 (1992).
[16] G. Stock, and W. Domcke, J. Opt. Soc. Am. B **7**, 1970 (1990).
[17] Y. J. Yan, L. E. Fried, and S. Mukamel, J. Phys. Chem. **93**, 8149 (1989).
[18] B. Fain, S. H. Lin, and N. Hamer, J. Chem. Phys. **91**, 4485 (1989).
[19] X. Z. Gu, M. Hayashi, S. Suzuki, and S. H. Lin, Biochim. Biophys. Acta **1229**, 215 (1995).
[20] Y. He, Y. Xiong, Z. Wang, Q. Zhu, and F. Kong, J. Phys. Chem. A **102**, 4266 (1998).
[21] L. Q. Dong, K. Niu, and S. L. Cong, Int. J. Quantum Chem. **107**, 1205 (2007).
[22] L. Q. Dong, K. Niu, and S. L. Cong, Chem. Phys. Lett. **432**, 286 (2006).
[23] L. Q. Dong, K. Niu, and S. L. Cong, Chem. Phys. Lett. **440**, 150 (2007).
[24] L. Q. Dong, K. Niu, and S. L. Cong, J. Theor. Comput. Chem. **6**, 885 (2007).
[25] K. Niu, L. Q. Dong, and S. L. Cong, J. Chem. Phys. **127**, 124502 (2007).
[26] S. Mukamel, *Principles of Nonlinear Optical Spectroscopy*, New York: Oxford University Press, (1995).
[27] L. Seidner, G. Stock, and W. Domcke, J. Chem. Phys. **103**, 3998 (1995).
[28] D. H. Schirrmeister and V. May, Chem. Phys. **220**, 1 (1997).
[29] V. May, Int. J. Quantum Chem. **106**, 3056 (2006).
[30] T. Mancăl and V. May, J. Chem. Phys. **114**, 1510 (2001).
[31] S. H. Lin, M. Hayashi, S. Suzuki, X. Gu, W. Xiao, and M. Sugawara, Chem. Phys. **197**, 435 (1995).
[32] B. Wolfseder and W. Domcke, Chem. Phys. Lett. **259**, 113 (1996).
[33] B. Wolfseder, L. Seidner, W. Domcke, G. Stock, M. Seel, S. Engleitner, and W. Zinth, Chem. Phys. **233**, 323 (1998).
[34] N. Balakrishnan, A. B. Alekseyev, and R. J. Buenker, Chem. Phys. Lett. **341**, 594 (2001).
[35] V. May and O. Kühn, *Charge Energy Transfer Dynamics in Molecular Systems,* Berlin: Wiley-VCH, (1999).
[36] S. M. Wang, K. J. Yuan, Y. Y. Niu, Y. C. Han, and S. L. Cong, Phys. Rev. A **74**, 043406 (2006).
[37] U. Kleinekathöfer, I. Kondov, and M. Schreiber, Chem. Phys. **268**, 121 (2001).
[38] D. Egorova, M. Thoss, W. Domcke, and H. Wang, J. Chem. Phys. **119**, 2761 (2003).
[39] M. V. Korolkov, J. Manz, and G. K. Paramonov, J. Phys. Chem. **100**, 13927 (1996).
[40] O. Kühn, D. Malzahn, and V. May, Int. J. Quantum Chem. **57**, 343 (1996).
[41] O. Kühn, V. May, and M. Schreiber, J. Chem. Phys. **101**, 10404 (1994).
[42] K. Blum, *Density Matrix Theory and Applications*, New York: Plenum, (1981).
[43] S. H. Lin, R. G. Alden, R. Islampour, H. Ma, and A. A. Villaeys, *Density Matrix Method and Femtosecond Processes*, Singapore: World Scientific, (1991).
[44] Z. Sun, Z. Jin, J. Lu, D. H. Zhang, and S. Y. Lee, J. Chem. Phys. **126**, 174104 (2007).
[45] A. G. Redfield, Adv. Magn. Reson. **1**, 1 (1965).
[46] T. I. Lai and E. C. Lim, Chem. Phys. Lett. **84**, 303 (1981).
[47] Y. Shi, Ph.D. Dissertation. Dalian: Chinese Academy of Sciences, No. B008003854, (2005).
[48] L. Randall and M. Therese, J. Phys. Chem. **94**, 3968 (1990).
[49] J. Y. Liu, Ph.D. Dissertation. Dalian: Chinese Academy of Sciences, No. B988003809, (2003).
[50] A. Kühl and W. Domcke, J. Chem. Phys. **116**, 263 (2001).

DOI:10.1088/1674-0068/21/03/211-216